JOURNAL OF MATERIALS SCIENCE 22 (1987) 818–825

Dislocation substructure in *in situ* deformed foils of niobium–8 to 10 at % vanadium alloy

Part 2

K. JAGANNADHAM
Materials Science and Engineering Department, North Carolina State University, Raleigh, North Carolina 27695, USA

FRANCIS C. LAABS
Metallurgy and Ceramics Division, Ames Laboratory, Ames, Iowa 50011, USA

The development of dislocation substructure in foils of niobium–8 to 10 at % vanadium alloy deformed *in situ* in the tensile stage of the microscope is presented to substantiate earlier observations presented in Part 1. The results of direct observation of the formation of straight dislocations, dislocation loops and loop debris are presented. In addition, the behaviour of cracks in foils containing hydrogen is compared with that observed in the absence of the interstitial. Through the *in situ* observations, the mechanism of embrittlement of niobium-rich vanadium alloys in the presence of hydrogen presented in Part 1 is substantiated.

1. Introduction

The development of dislocation substructure in the niobium–8 to 10 at % vanadium alloy has been described in Part 1 to determine the influence of hydrogen present in the interstitial sites in the lattice [1]. It has been demonstrated that cracks observed along active slip planes in the hydrogen-embrittled alloy single crystals are a result of early formation of dislocation cell walls. Further, accumulation of hydrogen along the cell walls leads to easier crack nucleation. On the other hand, the presence of straight long screw dislocations and edge segments is attributed to the effect of alloying by substitutional vanadium. In order to verify the above conclusions, foils of this alloy have been deformed *in situ* in the electron microscope and the results are presented in this paper.

Recent direct observation of thin foils of iron, of thickness less than 1 μm, deformed *in situ* in the tensile stage in an electron microscope equipped with an environmental cell has shown that cracks already present in the foils under constant tensile load moved due to the enhanced mobility of dislocations arising upon introducing hydrogen [2, 3], a solid softening effect. However, other authors [4] propose that the growing and changing concentration of hydrogen atmosphere drags the dislocations towards regions of the crack tip. On the other hand, enhanced dislocation motion is observed as an independent effect upon introducing hydrogen into the foils containing no cracks [2]. Yet another important and more direct local effect near the core of the dislocation will be the additional plastic strain introduced when hydrogen atoms accumulate and as a result give rise to tetragonal distortion associated with the interstitial. In fact, this effect similar to others will be proportional to the partial pressure of hydrogen at which it is introduced into the environmental cell, a result observed experimentally [2, 3] with the applied specimen displacement held constant. Further support to this contention is obtained from the fact that either helium or air did not have a similar effect since their diffusion into the foil is doubtful. In addition, the high mobility of hydrogen atoms and their interaction with the core of the screw dislocations can be responsible for their movement. Therefore, the observations of either dislocation movement or crack growth upon introduction of hydrogen with the foils under constraint may not be applicable to the situation when prior hydrogen charging is done. We do not intend to underscore the importance of charging the specimen under load in the environmental cell with hydrogen, since this may correspond to the actual situation encountered. On the other hand, it is our aim to emphasize the difference between the two categories of experiments, in particular when the solubility of hydrogen in iron is considered to be small [5].

In this respect, *in situ* experiments carried out on the niobium–8 to 10 at % vanadium alloy possessing a large interstitial solid solubility of hydrogen should be useful in understanding the effect of hydrogen. The trapping of hydrogen atoms to vanadium arising from either the electronic or the strain field interaction [6], which is responsible for the high hydrogen solid solubility in this alloy, is considered to prevent the hydrogen atoms from diffusing out of the foils tested in vacuum. In fact, it has been found that degassing of the previously charged specimens from hydrogen at 10^{-7} torr vacuum required raising the temperature above 400 to 500° C illustrating the tendency for hydrogen to remain within the specimens. The important parameter that seems to determine the nature of results obtained in the *in situ* experiments is the thickness of the foil [7]. It has been found that the very ductile metals show a brittle behaviour when the foil

0022–2461/87 $03.00 + .12

thickness is reduced below a certain limit. In this respect, the experiments performed on the niobium–vanadium alloy have comparable thickness when tested either with or without hydrogen. The operating voltage of the Jeol 100 CX electron microscope, in which the present experiments are carried out, is limited to 120 kV and as a result, the thickness of the foil that remained electron transparent is between 0.2 and 0.5 μm. In addition to the plane stress conditions in which the planes of maximum resolved shear stress different from those in plane strain, the constraints imposed by the free surfaces on the dislocation mobility can give rise to different results from those observed in the macroscopic specimens. On the other hand, the present observations will be useful in understanding the development of dislocation substructure and cracks in the presence of hydrogen at room temperature.

2. Experimental procedure

Specimens of niobium–8 to 10 at % vanadium alloy that can be pin loaded in tension, 8 mm × 3 mm × 1 mm in dimension were spark cut from a rolled foil. Further, the specimens were ground to 500 μm thickness, first on 320 grit followed by 600 grit silicon carbide papers and further electropolished to provide a smooth surface using an electrolyte of 6 vol % sulphuric acid in methanol. In order to start with an initially dislocation-free foil, the specimens were annealed for about 10 h at 1400° C under 10^{-7} torr vacuum. On the other hand, charging with hydrogen is done by taking the foils to 950° C at 10^{-6} torr vacuum and after isolating the furnace from the vacuum system, a premeasured volume of hydrogen from decomposition of uranium hydride is introduced into the furnace. The charging procedure is completed by keeping the specimens in a hydrogen atmosphere for 3 h and cooling the furnace. In addition, an electron transparent area of the foil is obtained in the centre of the specimen in the manner already mentioned in Part 1. The side entry eucentric stage, capable of single tilt about its axis by $\pm 55°$ and displacement controlled is used so that straining can be interrupted at any instant to record the observations. At the same time, a video camera has been placed in the front port and changes in the dislocation substructure as well as crack-related structure are recorded using a VCR. Instead of continuous loading of the foil, incremental elongation is carried out and between each increment, the structure is allowed to come to equilibrium. Several foils, both free of hydrogen and those containing hydrogen, have been deformed *in situ* in the transmission electron microscope. Some characteristic features of dislocation substructures observed are presented in this paper.

3. Initial substructure of the foils

The substructure in the annealed foils is relatively free from dislocations. On the other hand, all the dislocations present in the foil have rearranged in the form of sub-boundaries during annealing, as shown in Figs 1a and b. The structure of sub-boundaries changed its regularity whenever a lattice dislocation joined the boundary. In particular, the continuation of the lattice dislocation as part of a boundary dislocation should necessarily imply that the boundary is fairly coalesced [8]. These substructural features are not easily observed upon straining the foils by only a little. In other words, the lattice dislocations associated with the boundaries are found to be active sources provided the applied stress has a suitable component.

4. Dislocation substructure and slip line observations

The formation and development of slip lines and the associated dislocation lines is illustrated in Figs 2a and b as a function of increasing strain. In particular, the straight slip lines initially formed (Fig. 2a) increased in density and more were generated with increasing strain. In addition, the expanding dislocation configuration shown in Fig. 2b is similar to the observations presented in Part 1 (Fig. 3b). The fully developed straight dislocations in the top and the expanding dislocation configurations at several places in the composite picture (Fig. 2b) illustrate very clearly the higher lattice frictional stress resulting from the substitutional alloying of niobium with vanadium at room temperature. A schematic illustration of the expanding dislocations and the formation of straight screw dislocations in the foil subjected to tension, as shown in Fig. 2b is given in Fig. 2c. The shear stress component on the edge segments is responsible for the growing dislocations on each slip plane. The movement of dislocations schematically described in Fig. 2c is also illustrated in the micrographs shown in Figs 3a and b in which no cross slip is observed but extensive loop and debris formation is noticed (Fig. 3b). Furthermore, dislocations of opposite sign moving in the opposite direction can be seen in Fig. 3b. Thus, the left-hand side of the picture shows the dislocations moving up while the dislocations on the right are moving down; with the nature of the dark and light shades of contrast also reversed. The formation of loop debris in these foils and possibly in the macroscopic specimens could arise as a result of combination of positive and negative segments from the expanding dislocations in the opposite direction. A more direct evidence of this mechanism is seen in the dislocation substructure associated with a crack tip in a virgin crystal shown in Figs 4a and b. In addition, some moving segments curve around into a loop-like configuration and join together with another adjacent dislocation to form a complete loop. The dark and bright lobes of contrast associated with each terminating screw dislocation at the surface after completion of the loop formation can be seen [9]. These observations substantiate earlier conclusions of Part 1, on the effect of substitutional vanadium in increasing the lattice frictional stress to movement of both edge and screw dislocations.

5. Dislocation substructure associated with cracks

5.1. Foils containing no hydrogen

It has been pointed out earlier that the dislocation substructures observed in thinner foils are distinctly

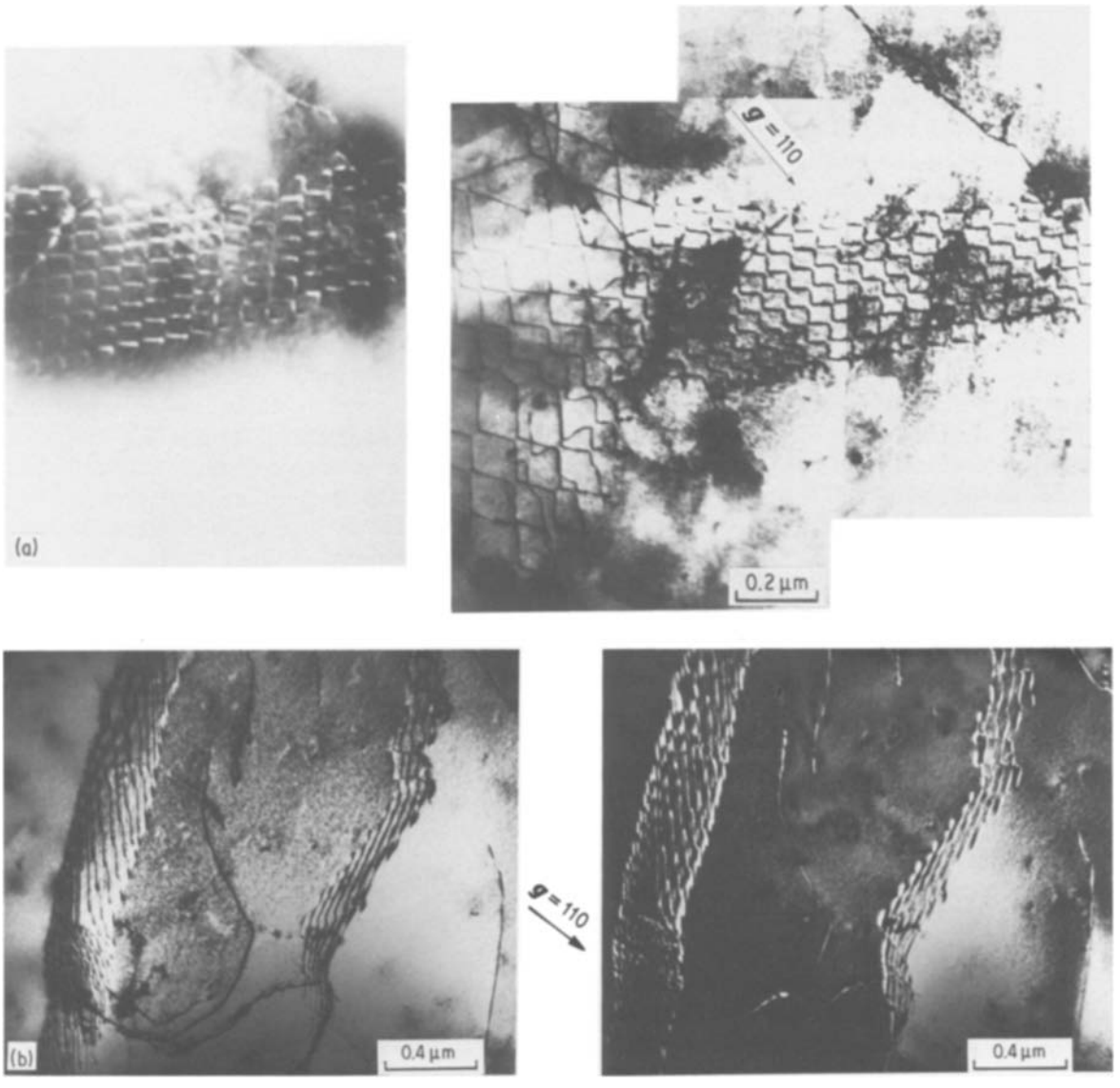

Figure 1 (a) and (b) Bright-field and centred dark-field (weak beam) electron micrographs of a sub-boundary observed in a well-annealed foil of niobium–10 at % vanadium alloy.

different from those observed in thicker foils. Thus, whereas substructures similar to those observed in macroscopic specimens are found in thicker samples, this is not true in thinner samples.

In particular, when the foil is deformed *in situ* in the microscope, the smaller size cracks present in the thinner area of the foil at the edge of perforation propagate into the thicker area of the foil which is not truly representative of the macroscopic specimens. The foils containing no hydrogen deformed very extensively in the absence of a crack at the edge. As a result of the plastic deformation, the foil is continuously thinned so that the nucleation of a small crack at the edge of the perforation can be observed as shown in Fig. 5a. The crack tip has a very thin area ahead of it within which no dislocation substructure can be observed other than the bend contours, but surrounding it the dense dislocation substructure is observed. Further crack growth takes place when the foil area containing the dense dislocation substructure becomes thinner [10] and the crack in the thinner area moves forward by the nucleation of a slit in front and its coalescence with the crack [11] as shown in Fig. 5b. Small sub-micrometre size holes formed in the thinned area of the foil ahead of the crack tip are also observed [12] in Fig. 5b. Further extension of the sample leads to the opening of the crack surfaces while thinning the area ahead, as shown in Fig. 5c. Eventually, when the crack enters the thicker area of the foil, extensive plastic deformation in the region ahead of the crack tip blunts the crack as shown in Fig. 5d. While the above description of the crack growth is suitable for foils of 0.3 to 0.5 μm thickness of this alloy with no hydrogen, Fig. 6 illustrates another crack inclined to the tensile axis which propagated with very little deformation. The thinned area of the foil surrounding the hair line crack is also shown. On the other hand, extensive plastic deformation that is present at the tip of a crack which is subject to a shear stress parallel to the crack faces along its length in the foil is shown in Fig. 7. The plastic zone on one side of the crack is prevented from spreading by bands of deformation such as those described earlier in Part 1 (Fig. 5).

5.2. Foils containing hydrogen

In order to determine the behaviour of cracks in foils

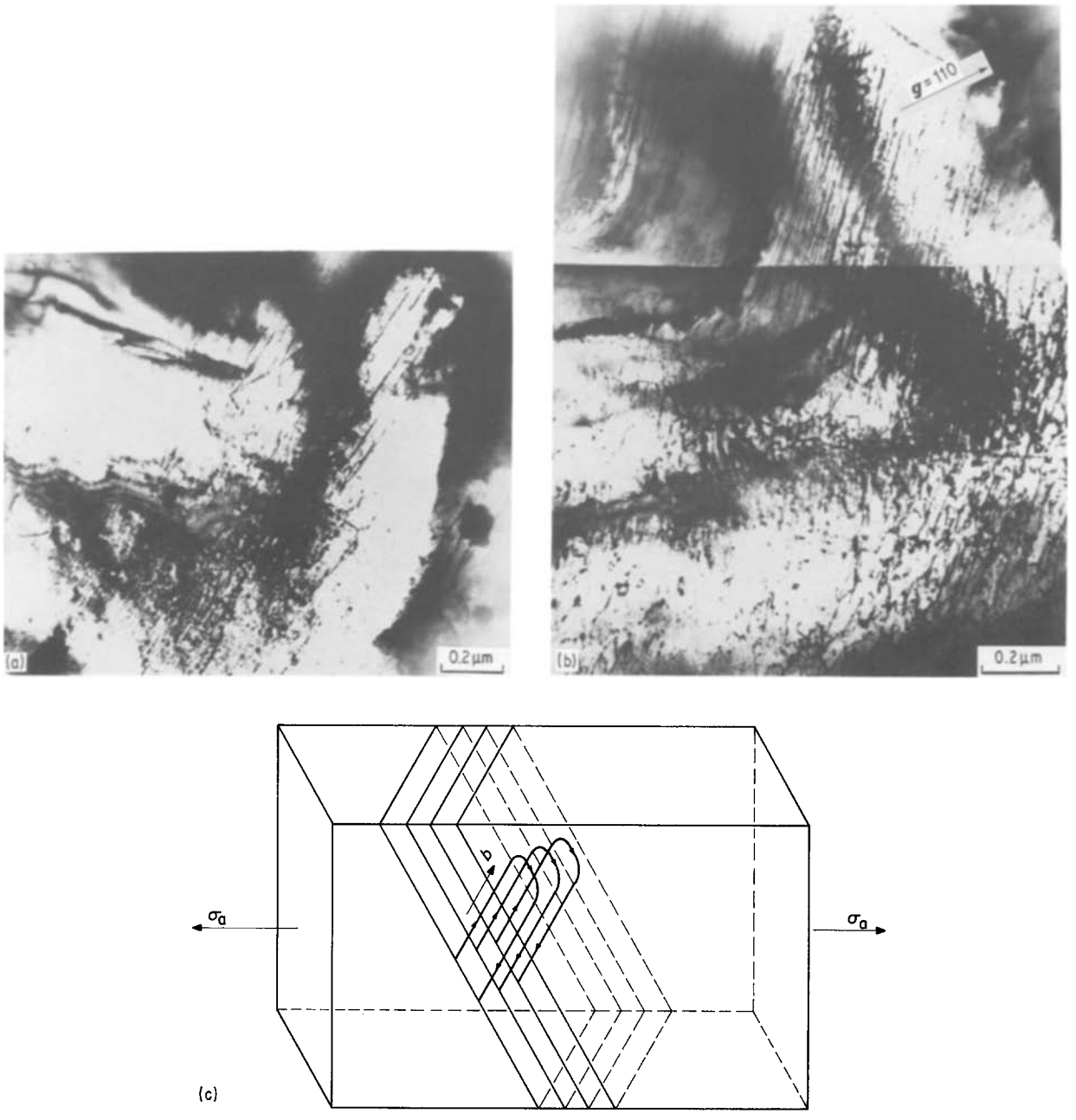

Figure 2 (a) Long parallel dislocations and development of slip traces observed after an initial deformation of the foil of niobium–10 at % vanadium alloy *in situ* in the tensile stage. (b) Long straight screw dislocations formed in a foil of niobium–10 at % vanadium alloy deformed *in situ* in a tensile stage. (c) A schematic illustration of the formation of straight long screw dislocations in the foil deformed *in situ* in the tensile stage.

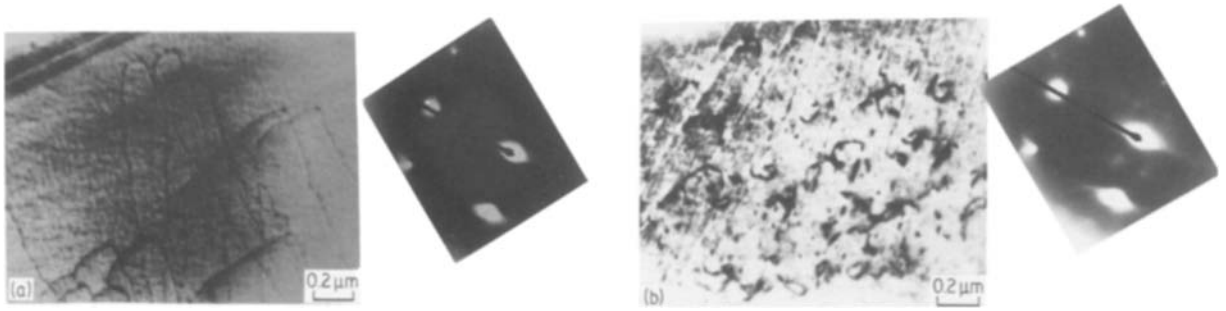

Figure 3 (a) Dislocation movement, and (b) dislocation movement and loop debris, observed in a well-annealed foil of niobium–10 at % vanadium alloy deformed *in situ* in a tensile stage.

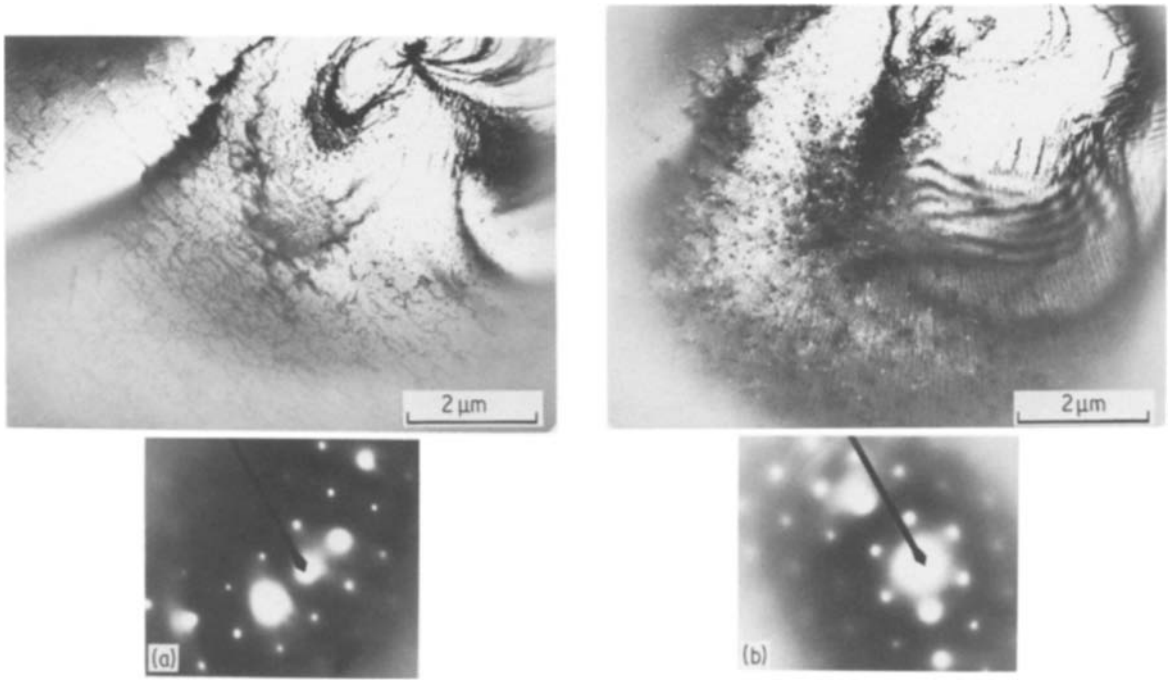

Figure 4 (a) Dislocation loop formation from dislocations of opposite sign formed in front of a crack tip in a virgin crystal of niobium–10 at % vanadium alloy. (b) Dark and light lobes associated with screw dislocations ending at the free surface. The dislocation substructure corresponds to the area in front of a crack tip shown in (a).

of comparable thickness in the presence of hydrogen, a few foils charged with 200 p.p.m. wt % hydrogen have been deformed *in situ* in the tensile stage. The substructural changes which are typically associated with a crack at various stages of incremented specimen elongation are illustrated in Figs 8a to e. Upon a small elongation imposed on the specimen (Fig. 8a), the crack initially present in the foil extended with slip on two planes equally inclined to the symmetrical crack line generating ledge steps on the crack faces. The direct correspondence between the glide planes and the ledge steps separating the crack faces is apparent. At the same time, the sharpness of the crack remained with extensive dislocation substructure developed in order to relieve the stress concentration at the tip. The crack has by now entered into a relatively thicker area of the foil. The slip lines and the arrangement of straight dislocations with loop debris seen in Fig. 8b indicate that the foil deformation independent of the crack is superimposed on that associated with the crack-tip forming ledge steps. Furthermore, there is extensive multiplication along the symmetry line forming a dense dislocation network and a more rounded crack tip compared to the earlier sharp configuration. The extensive dislocation multiplication directly ahead of the crack is considered to be the result of hydrogen-induced mobility of dislocations which is absent in other foils. Further extension was responsible for the opening of the crack surfaces and rounding of the crack tip with a small circular area ahead of the tip becoming thinner and more electron transparent (Fig. 8c). Specifically, the small circular area is formed in a region with dense dislocation substructure. However, with further thinning, the circular area becomes free from dislocation substructure and finally a hole is seen to form (Fig. 8d). It is important to note that the crack, while opening up to a larger radius at the tip, has not extended from its two previous positions. Similar crack growth behaviour has been observed in several foils containing hydrogen, although the circular nature of the hole is generally replaced by an irregular hole. A comparison of these observations with the crack growth behaviour in the absence of hydrogen atoms shows that the nucleation of a hole in front of the crack tip within the dense dislocation substructure formed in the presence of enhanced dislocation mobility due to hydrogen is the characteristic difference. The uniform thinning of the foil in the region ahead of the tip observed in the specimens without hydrogen is conspicuously absent in the foils with hydrogen. The coalescence of the crack tip with the hole finally was responsible for the configuration which is very much rounded and blunt (Fig. 8e). Further, the substructural features of dislocations on two slip systems associated with the crack are easily observed in the foil area.

6. Discussion and conclusions

The observations of the foils deformed *in situ* in the tensile stage at room temperature have provided clear evidence of the formation of straight dislocations and loops in this alloy supporting earlier conclusions of Part 1. On the other hand, it is thought that the formation of dislocation cell structure in the presence of hydrogen cannot be observed unless much thicker samples are examined. At present, it is believed that the constraints imposed by the surface in the thinner foils restricts the mobility of dislocations to rearrange into low energy configurations.

The growth of cracks in the electron transparent foil is also very much influenced by the thickness, becoming much closer to the behaviour observed in macroscopic specimens when foil areas of larger thickness are under observation. On the other hand, the

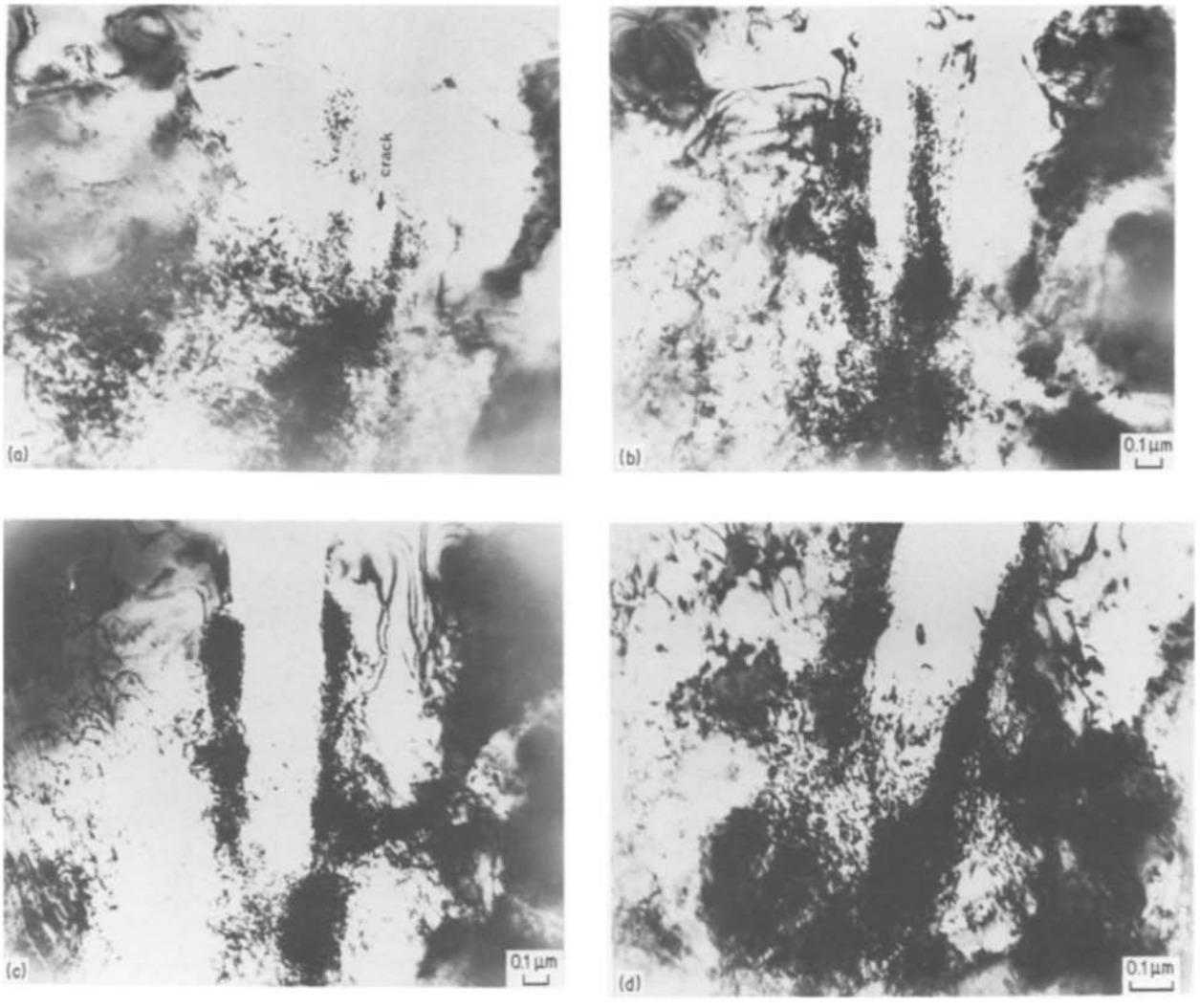

Figure 5 (a) Crack nucleation in a region of high dislocation density observed close to the edge of the foil of niobium–10 at % vanadium alloy deformed *in situ* in the tensile stage of the microscope. Multiple $\boldsymbol{g}$ vectors are operating. (b) A well defined tensile crack with surrounding dislocation substructure formed after further deformation of the foil of niobium–10 at % vanadium alloy *in situ* in the tensile stage. Multiple $\boldsymbol{g}$ vectors are operating. (c) Crack growth with surrounding dislocation substructure observed after further deformation of the foil of niobium–10 at % vanadium alloy *in situ* in the tensile stage. Multiple $\boldsymbol{g}$ vectors are operating. (d) Crack tip blunting due to extensive deformation and formation of dislocation substructure surrounding the crack in the foil of niobium–10 at % vanadium alloy deformed *in situ* in the tensile stage. Multiple $\boldsymbol{g}$ vectors are operating.

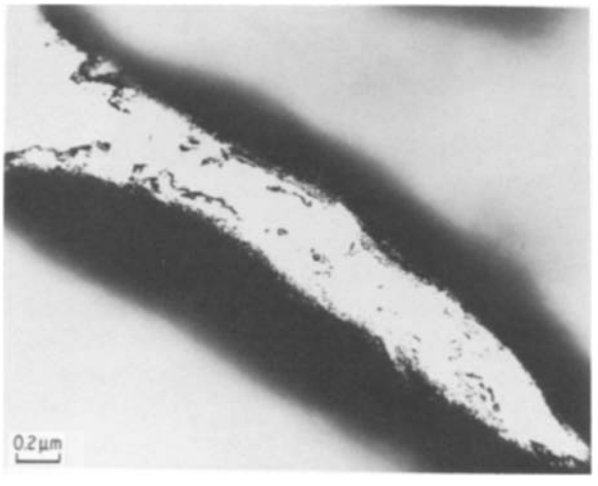

Figure 6 Crack propagation with very little plastic deformation in the surrounding regions around the tip observed in a foil of niobium–10 at % vanadium alloy deformed *in situ* in the tensile stage.

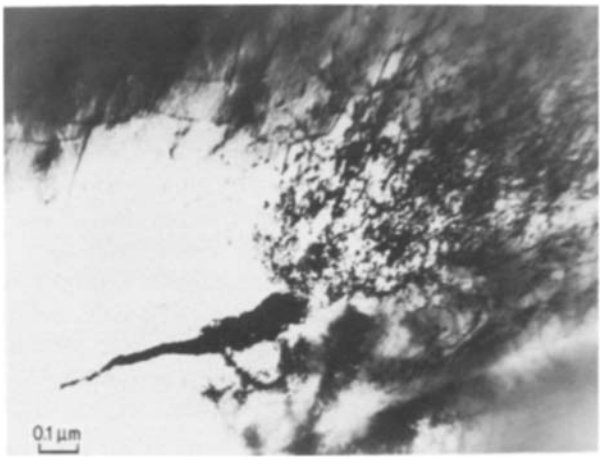

Figure 7 Dislocation substructure formed ahead of the crack tip in a foil of niobium–10 at % vanadium alloy deformed *in situ* in the tensile stage. The crack is subject to a shear stress parallel to the crack faces. Multiple $\boldsymbol{g}$ vectors are operating.

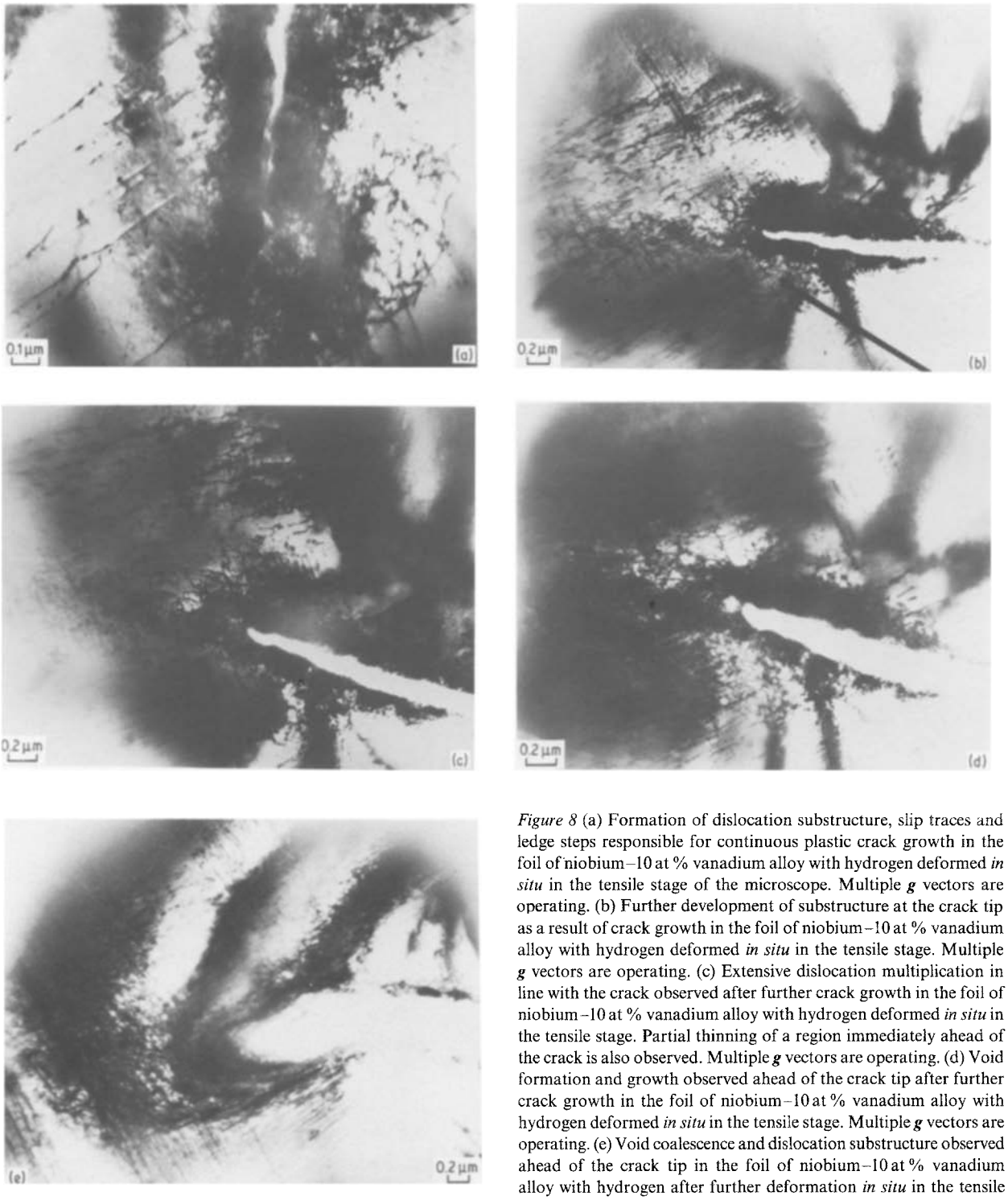

Figure 8 (a) Formation of dislocation substructure, slip traces and ledge steps responsible for continuous plastic crack growth in the foil of niobium–10 at % vanadium alloy with hydrogen deformed *in situ* in the tensile stage of the microscope. Multiple $\boldsymbol{g}$ vectors are operating. (b) Further development of substructure at the crack tip as a result of crack growth in the foil of niobium–10 at % vanadium alloy with hydrogen deformed *in situ* in the tensile stage. Multiple $\boldsymbol{g}$ vectors are operating. (c) Extensive dislocation multiplication in line with the crack observed after further crack growth in the foil of niobium–10 at % vanadium alloy with hydrogen deformed *in situ* in the tensile stage. Partial thinning of a region immediately ahead of the crack is also observed. Multiple $\boldsymbol{g}$ vectors are operating. (d) Void formation and growth observed ahead of the crack tip after further crack growth in the foil of niobium–10 at % vanadium alloy with hydrogen deformed *in situ* in the tensile stage. Multiple $\boldsymbol{g}$ vectors are operating. (e) Void coalescence and dislocation substructure observed ahead of the crack tip in the foil of niobium–10 at % vanadium alloy with hydrogen after further deformation *in situ* in the tensile stage. Multiple $\boldsymbol{g}$ vectors are operating.

fundamental crack-tip phenomena are easily observed in moderately thick samples such as those employed in the present experiments. While many features are common to the crack tip and the surrounding substructure in specimens either containing hydrogen or not, the nucleation and coalescence of a hole of submicrometre size ahead of the tip in the region containing dense dislocation substructure is considered as a distinct mechanism of hydrogen embrittlement which is considered common to macroscopic specimens as well. Thus the quasi-brittle behaviour in which crack propagation through void nucleation and coalescence takes place is identified as the mechanism of hydrogen embrittlement. The nucleation of a slit ahead of, but not at, the crack tip in the thinned area of the foil is not surprising since the stress field associated with a plastic crack under small scale yielding has been found to reach a singularity away from the tip [11, 13]. Recent numerical calculations have illustrated that nucleation of a slit ahead of a plastic crack tip is energetically favourable [11] provided the crack length is sufficiently large and the material is quasi-brittle.

Acknowledgements

This work was performed for the United States Department of Energy, Office of Basic Energy Sciences, Division of Materials Sciences under contract number: W-7405-Eng-82. This manuscript was presented at the

Symposium on Refractory Metals at the AIME Fall Meeting of 1984, Detroit, Michigan.

References

1. K. JAGANNADHAM and FRANCIS C. LAABS, *J. Mater. Sci.* **22** (1987) 803.
2. T. TABATA and H. K. BIRNBAUM, *Scripta Metall.* **18** (1984) 231.
3. *Idem, ibid.* **17** (1983) 947.
4. J. KING and B. BLOCK, *ibid.* **19** (1985) 337.
5. J. P. HIRTH, *Met. Trans.* **11A** (1980) 861.
6. J. F. MILLER and D. C. WESTLAKE, *Trans. Jpn. Inst. Metals* **21** (1980) 153.
7. H. G. F. WILSDORF, *Mat. Sci. Engng* **59** (1983) 1.
8. K. JAGANNADHAM and M. J. MARCINKOWSKI, "Unified Theory of Fracture" (Trans Tech SA, Switzerland, 1983).
9. P. B. HIRSCH, R. B. NICHOLSON, A. HOWIE, D. W. PASHLEY and M. J. WHELAN, "Electron Microscopy of Thin Crystals" (Butterworths, London, 1965) Ch. 11, p. 275.
10. J. A. HORTON and S. M. OHR, *J. Mater. Sci.* **17** (1982) 3140.
11. K. JAGANNADHAM, *Mat. Sci. Engng* **60** (1983) 95.
12. T. C. POLLOCK and H. G. F. WILSDORF, *ibid.* **61** (1983) 7.
13. G. R. IRWIN and M. F. KOSKINEN, *Trans. ASME.* **85D** (1963) 593.

Received 13 November 1985
and accepted 30 June 1986